

# **JGR** Oceans

#### RESEARCH ARTICLE

10.1029/2024JC021438

### **Key Points:**

- Superoxide maxima consistently appear in dark waters below the mixed layer
- Corresponding dips in oxygen at depths of superoxide maxima suggest link between heterotrophic respiration and superoxide production

#### **Supporting Information:**

Supporting Information may be found in the online version of this article.

#### Correspondence to:

C. M. Hansel, chansel@whoi.edu

#### Citation:

Taenzer, L., Pardis, W., Wankel, S. D., Kolbe, M., Voss, M., Schulz-Vogt, H., et al. (2024). Subsurface superoxide spans the Baltic Sea. *Journal of Geophysical Research: Oceans*, 129, e2024JC021438. https://doi.org/10.1029/2024JC021438

Received 7 JUN 2024 Accepted 22 SEP 2024

#### **Author Contributions:**

D. Wankel, Colleen M. Hansel
Data curation: Heide Schulz-Vogt
Formal analysis: Lina Taenzer, Colleen
M. Hansel
Funding acquisition: Dalton S. Hardisty,
Colleen M. Hansel
Investigation: Lina Taenzer,
William Pardis, Martin Kolbe,
Heide Schulz-Vogt, Christian Burmeister,

Conceptualization: Lina Taenzer, Scott

Colleen M. Hansel
Methodology: Lina Taenzer,
William Pardis, Scott D. Wankel,
Martin Kolbe, Colleen M. Hansel
Project administration: Colleen

M. Hansel

Resources: Maren Voss, Colleen

M. Hansel

Software: William Pardis Supervision: Colleen M. Hansel Writing – original draft: Lina Taenzer

© 2024. The Author(s). This is an open access article under the terms of the Creative Commons Attribution License, which permits use, distribution and reproduction in any medium, provided the original work is properly cited.

# Subsurface Superoxide Spans the Baltic Sea

Lina Taenzer<sup>1,2</sup>, William Pardis<sup>3</sup>, Scott D. Wankel<sup>1</sup>, Martin Kolbe<sup>4</sup>, Maren Voss<sup>4</sup>, Heide Schulz-Vogt<sup>4</sup>, Christian Burmeister<sup>4</sup>, Dalton S. Hardisty<sup>5</sup>, and Colleen M. Hansel<sup>1</sup>

<sup>1</sup>Marine Chemistry and Geochemistry, Woods Hole Oceanographic Institution, Woods Hole, MA, USA, <sup>2</sup>Earth, Atmospheric and Planetary Sciences, Massachusetts Institute of Technology, Cambridge, MA, USA, <sup>3</sup>Woods Hole Oceanographic Institution, Applied Ocean Physics and Engineering, Woods Hole, MA, USA, <sup>4</sup>Leibniz Institute for Baltic Sea Research Warnemünde, Rostock, Germany, <sup>5</sup>Department of Earth and Environmental Sciences, Michigan State University, East Lansing, MI, USA

**Abstract** Superoxide is a reactive oxygen species that is influential in the redox chemistry of a wide range of biological processes and environmental cycles. Using a novel in situ sensor we report the first water column profiles of superoxide in the Baltic Sea, at concentrations higher than previously observed in other oceans. Our data revealed consistent peaks of superoxide (2.0–15.1 nM) in dark waters just below the mixed layer. The oxic waters, low metal concentrations, and lack of sunlight imply that the peak is likely of biological origin. Several profiles displayed a concomitant dip in dissolved oxygen mirroring this superoxide peak, strongly suggesting a link between the two features. The magnitude and distribution of superoxide observed warrants re-evaluation of the most relevant sources and controls of superoxide in seawater. Locally, these high concentrations of superoxide may create environments conducive to reactions with trace metals and organic matter and present an overlooked sink of oxygen in the Baltic Sea.

**Plain Language Summary** The combination of unusual inflow activity and topographic conditions with strong anthropogenic influence in the Baltic Sea, offer a unique environment to study redox chemistry. To gain further insight into the biogeochemical cycles in this area we made the first measurements of superoxide, a reactive oxygen species that plays significant roles in organismal health, as well as the chemistry of metals and carbon in seawater. We made direct measurements of superoxide in seawater, leading to continuous profiles between 2 and 80 m at 7 different locations in the Baltic Sea. Our results revealed the presence of widespread superoxide maxima that consistently appeared in dark waters at depths between 23 and 35 m. In some instances, the superoxide peaks are mirrored by dips in oxygen concentrations. This work demonstrates that light-independent processes were the dominant source of superoxide in the Baltic Sea in September, and point to an association between heterotrophic activity, oxygen loss, and superoxide production. The high levels of superoxide observed in this study suggest that a reevaluation of the abundances of this compound in seawater is necessary, and underline the advantages of in situ techniques for capturing total superoxide concentrations.

# 1. Introduction

The unique ecosystem of the Baltic Sea is shaped by a combination of unusual topographic and hydrographic conditions (Matthäus & Franck, 1992). The sole input of saline water is through the Danish Straits which sporadically injects seawater from the North Sea into the Baltic Sea. Due to the high volume of riverine water, and limited inflow of seawater, the Baltic Sea is one of the largest brackish water bodies in the world (Ojaveer et al., 2010). The brackish surface layer which spans the euphotic zone is stratified from the deeper more saline waters at depths of around 60–80 m in the Baltic Proper and limits deep water ventilation. Eutrophication has enhanced this oxygen deficiency already present due to poor ventilation, resulting in anoxic bottom waters and accumulation of hydrogen sulfide (Carstensen et al., 2014).

The steep oxygen gradients that characterize the Baltic Sea provide a singularly opportune setting to study elemental redox coupling. A wealth of previous studies has highlighted the dynamic cycles of Fe and Mn, and interactions with P and other trace metals (e.g. Co, Mo, U, V, and W) (Dellwig et al., 2010; Hermans et al., 2019; Laima et al., 2001; van de Velde et al., 2020). The rapid cycling between metal oxidation states, and reactions with nutrients and organic matter suggest an environment conducive to the production of reactive intermediates that may persist at low concentrations but have high fluxes.

TAENZER ET AL. 1 of 15

#### Writing – review & editing: Lina Taenzer, Scott D. Wankel, Maren Voss, Heide Schulz-Vogt, Dalton S. Hardisty, Colleen M. Hansel

Superoxide ( ${\rm O_2}^{-\bullet}$ ), is a reactive oxygen species (ROS) that is formed by the single electron reduction of molecular oxygen. The abundance and distribution of ROS in surface and deep-sea waters have widespread implications. ROS can play critical roles in the cycling of carbon, and redox-sensitive metals such as copper, iodine, iron, and manganese (Archibald & Fridovich, 1982; Hansard et al., 2011; Heller & Croot, 2010b; Learman et al., 2013; Li et al., 2014; Luther, 2023; Rose, 2012; Wuttig et al., 2013). Recent work has further shown that superoxide production can act as a net sink of dissolved oxygen in the water column, underlining its importance in oxygen dynamics in both the light and dark ocean (Sutherland, Wankel, & Hansel, 2020). Organismal health can be influenced in either positive or negative manners by ROS levels. At regulated levels, superoxide plays essential roles in the function of higher eukaryotes (Aguirre et al., 2005; Lamb & Dixon, 1997) and recent work has implicated ROS (specifically  ${\rm H_2O_2}$ ) in beneficial processes for microbes spanning from cell signaling to growth (Buetler et al., 2004; Diaz et al., 2019; Hansel et al., 2019; Roe & Barbeau, 2014). Logically, in a system as dynamic and redox stratified as the Baltic Sea, superoxide may play a heightened role in microbial ecology and biogeochemistry and provide an unparalleled natural site to study its water column dynamics.

Canonically, the main source of superoxide production in the ocean has been attributed to an abiotic photochemical process, specifically via the photolysis of colored dissolved organic matter (CDOM) (Garg et al., 2011; Powers & Miller, 2014; Shaked & Armoza-Zvuloni, 2013). However, a series of key discoveries in the last decades reveal the importance of enzyme and metabolite-mediated biological production and have led to a new framework for understanding of marine superoxide production. Superoxide can be generated by heterotrophs and phytoplankton (Diaz et al., 2013; Sutherland et al., 2019), with the potential for light independent production appearing to be widespread across these micro-organisms (Diaz et al., 2019; Yuasa et al., 2020). The decrease in superoxide concentration upon removal of particles from natural waters in the dark suggests a likely microbial origin for this ROS (Roe et al., 2016; Rose et al., 2008; Zhang et al., 2016). Despite this progress in understanding of marine ROS, we still lack a basic understanding of the distribution of superoxide within the water column and how this relates to patterns in light, oxygen, temperature, nutrients, and microbial community composition.

The short half-life of superoxide in seawater (typically between seconds and minutes) (Petasne & Zika, 1987) has historically complicated efforts to quantify superoxide in seawater. Consequently, earlier efforts to characterize superoxide in the water column have largely used decay rates to back-calculate concentrations (Hansard et al., 2010; Rose et al., 2008; Rusak et al., 2011), or relied on evaluating specific production pathways from assessments of particle-associated and non-particle associated waters (Roe et al., 2016; Schnur et al., 2024; Sutherland, Grabb, et al., 2020). As a result, our understanding of the true abundances and distributions of superoxide in seawater is highly limited, with very poor spatial or temporal resolution. Yet, advancing our knowledge of superoxide dynamics may provide a new lens through which to study biogeochemical cycles, particularly in highly stratified systems such as the Baltic Sea that are increasingly subject to anthropogenic influence. Here we leveraged a novel in situ sensor to provide the first characterizations of superoxide throughout the water column of the Baltic Sea, adding a new dimension through which to describe the unique biogeochemistry of this sea.

### 2. Materials and Methods

#### 2.1. Sampling Stations

Data were collected during a research cruise (EMB276) on the R/V Elisabeth Mann Borgese from September 20 to September 27 of 2021. Seven different stations in and around the eastern Gotland Basin were studied (Figure 1). A list of the locations by latitude and longitude is given in Table S1 of Supporting Information S1.

# 2.2. Superoxide Analysis

In situ measurements of superoxide were made using a recently developed superoxide sensor (SOLARIS), which has been previously described in detail (Taenzer et al., 2022). Briefly, SOLARIS quantifies superoxide using a chemiluminescent method. Seawater is drawn in continuously through a sampling wand and combines with the chemiluminescent probe methyl *Cypridina* luciferin analog (MCLA) in a mixing cell (see Table 1). MCLA reacts specifically with superoxide producing light which is quantified by a photomultiplier tube. Operation of SOLARIS, including manipulation of pump speeds, and choice of program (calibration or environmental measurement) is handled through a custom user interface in real time during deployments. Data are collected as raw counts, at the frequency of 2 Hz, which depending on the speed of the CTD descent equates to a continual profile

TAENZER ET AL. 2 of 15

2169291, 2024, 10, Downloaded from https://agupubs.onlinelibrary.wiley.com/doi/10.1029/2024JC021438 by Michigan State University, Wiley Online I

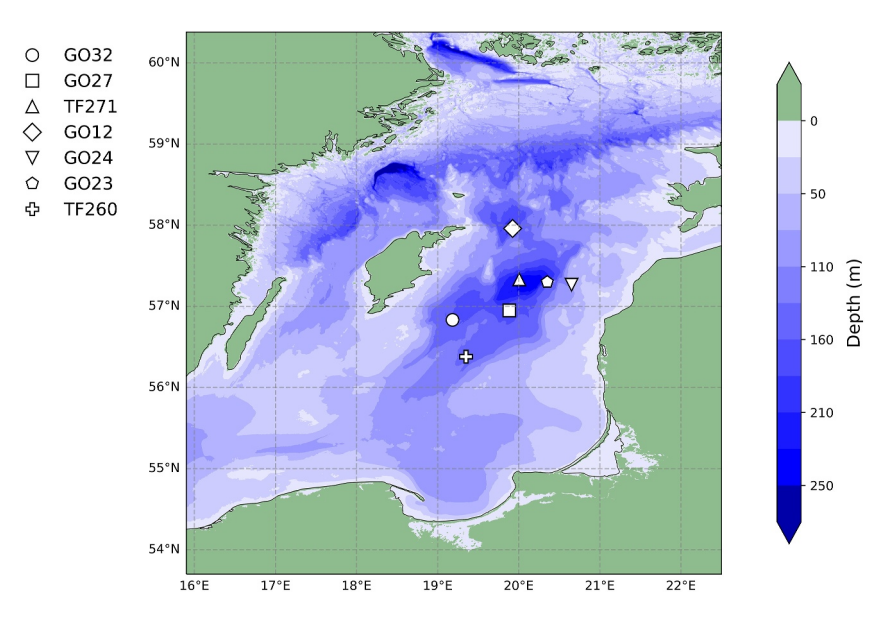


Figure 1. A map illustrating the depth (in meters) of the Baltic Sea. Sampling stations are shown by different symbols.

with 8–15 data points per meter. During deployments the instrument is run in one of three modes: (a) analysis of seawater (pump speeds: MCLA 6.2 mL/min, seawater via sampling wand 6.2 mL/min), (b) background correction (pump speeds: MCLA 6.25 ml/min, seawater via sampling wand 4.75 mL/min, SOD 1.5 mL/min), or (c) calibration (toggles between three stages, a. MCLA 6.25 mL/min, BGSW 6.25 mL/min, b. MCLA 6.25 mL/min, BGSW 4.75 mL/min, SOTS 1.5 mL/min, and c. MCLA 6.25 mL/min, BGSW 4.75 mL/min, SOTS 1.5 mL/min, SOD 1.25 mL/min).

SOLARIS signals are calibrated using a solution of superoxide thermal source (SOTS-1), based on methods outlined previously (Heller & Croot, 2010c; Taenzer et al., 2022). SOTS-1 degrades and yields superoxide at a highly constrained, temperature-dependent rate. To control the temperature component of the degradation rate as SOLARIS moves along temperature gradients in the water column, SOTS-1 is stored within a thick-walled, temperature-regulated, acrylic chamber on SOLARIS. The SOTS-1 chamber is filled with water that is maintained at a temperature of 26°C. All other reagents, and the sampled seawater is at ambient temperature. SOTS-1 solutions (100  $\mu$ M) were prepared eight hours prior to deployments to target steady-state concentrations in the SOTS-1 as described by others (Heller & Croot, 2010c). The chemiluminescent probe MCLA, was prepared from frozen stock solutions prior to the start of each deployment, as was a solution of superoxide dismutase (SOD), which degrades superoxide and is thus used to verify that the photon signal is responding to superoxide in seawater. Solutions are filled into sterile plastic bags (Thermo Scientific, Latiner P/N SH3071403, 0.5 or 2L volumes) with the use of 60 mL plastic syringes. Any air bubbles are removed from the reagent bags before being put into place on SOLARIS.

In this study, SOLARIS was mounted to the frame of a rosette on which it traveled vertically through the water column. As a result, measurements begin at 2 m depth, and there were no measurements made directly at the sea surface. As it takes roughly 28 s for the seawater to travel from the tip of the sampling wand to the flow cell where the signal is recorded, the signals are time-adjusted to match the depths of the CTD 28 s prior to the raw count

**Table 1**Table of Reagents Used in Superoxide Quantifications on SOLARIS

Solution	Concentration	Purpose	
MCLA	4 μΜ	Chemical probe, generates signal upon reaction with superoxide	
Superoxide thermal source (SOTS-1)	100 μΜ	Superoxide standard, decomposes to produce superoxide	
Superoxide Dismutase (SOD)	~6 kU/200 mL	Verifies superoxide signal	
Background Seawater	Filtered + amended to a final concentration of 75 $\mu M$ DTPA	Baseline signal for calibrations	

TAENZER ET AL. 3 of 15

signal read. The rosette was regularly stopped during its descent through the water column to allow for determination of depth and temperature specific calibration factors, which were then used to convert raw photon counts to superoxide concentrations. The reagent body of SOLARIS is tightly enclosed in an opaque sheet of black plastic, that shields it from the light.

#### 2.3. Analysis of Associated Parameters

Temperature, oxygen, salinity, photosynthetically active radiation (PAR) (Biospherical Instruments Inc.), fluorescence (WETStar Fluorometer), and turbidity (ECO FLNTU) were measured on a standard CTD package and associated rosette mounted sensors (Seabird 9/11+, SN-911+). Macronutrients (PO<sub>4</sub><sup>3-</sup>, NO<sub>3</sub>, NO<sub>2</sub><sup>-</sup>, and NH<sub>4</sub><sup>+</sup>) as well as pH, silica, and hydrogen sulfide were obtained via microsensors and a constant flow analyzer (QuAAtro Seal analytical) in line with an independent pump CTD as described by Strady et al. (2008) and Schulz-Vogt et al. (2019). Nutrient analysis followed guidelines of Grasshoff et al. (1999) and HELCOM (2017), with the precision on each nutrient being 0.01 (PO<sub>4</sub><sup>3-</sup>), 0.02 (NO<sub>3</sub><sup>-</sup>), 0.006 (NO<sub>2</sub><sup>-</sup>), and 0.05 (NH<sub>4</sub><sup>+</sup>) μM. Due to time constraints, the pump CTD profile focused exclusively on the depth range of the chemocline, typically falling between 30 and 50 m, and proceeded downward. As a result, these parameters were not characterized in surface and near-surface waters.

#### 2.4. Calculation of Superoxide Production Rates

Assuming steady-state, the production of superoxide in seawater must be balanced by its decay rate. Thus, the production rate  $(P_{O2-})$  in nmol  $L^{-1}$   $h^{-1}$  is given as:

$$P_{O2-} = [O_2^-] \times k \times 3600$$

Where the  $[O_2^-]$  is given in nM, and k is the decay rate constant in s<sup>-1</sup>. In natural waters, decay constants of superoxide typically range between 0.002–0.016 s<sup>-1</sup> (Hansard et al., 2010). However, as superoxide is known to also react with organic matter (Heller & Croot, 2010a), the humic rich nature of the Baltic Sea (Osburn & Stedmon, 2011; Terzic et al., 2024) would likely be characterized by a higher decay rate than in typical seawater.

# 2.5. Statistical Analysis

Data normality and homogeneity of variance were first assessed using Levene's test prior to further statistical analyses. Relationships between station location, thermocline depth, concentrations, depths of subsurface peaks, and fluorescence were tested using a one-way analysis of variance (ANOVA) or bivariate fits. JMP (version 16.2.0) was used for all statistical analyses.

### 3. Results

#### 3.1. Meteorology and General Water Column Characteristics

Direct meteorological data, including air temperature, wind speed, and humidity from the sampling stations were captured by the ship's onboard sensors. Air temperatures in the timeframe between September 20th and September 27th varied between 10.0 and 16.8 (°C) (Table S1 in Supporting Information S1). Some precipitation occurred on September 23rd and September 24th, but all other days were dry. The sampling period was characterized by inconsistent wind speeds, alternating from fairly high at the start of the sampling period (8.8 m s $^{-1}$ ) on September 20th followed by a drop in winds (reaching 4.6 m s $^{-1}$ ) on September 22nd, after which it rose again (8.5 m s $^{-1}$ ) by September 23rd. The lowest mean wind speed was observed on September 26th (3.9 m s $^{-1}$ ), and then picked up again on September 27th (9.6 m s $^{-1}$ ). The depth of the euphotic zone, defined as the depth at which just 1% of the surface PAR remains, varied between 10 and 24 m between different stations and time of day (see Table 2).

As seen in Figure 2, the different stations varied in their oxygen, turbidity, and fluorescence profiles. Oxygen was near-saturation with the atmosphere at 2 m (280–300  $\mu$ M) and rapidly began to decline around 60–65 m separating oxygenated surface waters from sulfidic bottom waters by 75–90 m (see Figure S1 in Supporting Information S1). Within the oxic water column, station TF271 showed the highest amount of fluctuation in the oxygen profile between 20 and 50 m depth. GO23 displayed some variability in this region as well, but the oscillations

TAENZER ET AL. 4 of 15

 Table 2

 The Time of Each Cast at Different Stations Along With the Near Surface Superoxide Concentrations (at 2 m), and the Depth and Concentration of the Superoxide Peak

Station	Time	$O_2^-$ (nM) at 2 m	Surface PAR	Depth of O <sub>2</sub> <sup>-</sup> peak (m)	O <sub>2</sub> peak (nM)	1% PAR depth
GO27	06:22	2.3	21.00	29	9.6	20
TF271	04:07	6.4	0.37	31	7.8	18
TF271	13:04	7.6	21.00	25	9.6	19
TF271	17:30	2.9	21.00	23	10.1	19
GO12	03:12	3.8	0.40	23	6.1	10
GO24	03:26	2.3	0.33	30	6.5	10
GO24	04:41	1.6	2.39	27	4.2	13
GO23	10:08	2.4	175.88	27	2.7	16
GO23	12:05	3.5	182.99	30	2.2	15
GO23	13:01	2.5	114.34	31	2.0	15
TF260	05:31	6.0	6.32	32	15.1	24
TF260	07:14	2.1	14.56	31	9.7	24
TF260	11:57	2.7	105.71	29	8.7	19
TF260	12:58	1.7	118.30	35	6.7	10
GO32	13:04	2.0	21.60	24	4.2	20

Note. The depth of the euphotic zone is given as the depth at which 1% of the surface PAR is reached.

occurred on a smaller amplitude than at TF271. In many of the casts, local dips in oxygen were seen at a depth around 24 m, below the mixed layer depth. A drop in oxygen at this depth was most defined at casts at GO27 (dropping from 280 to 200 µM), TF260 (280 to 216 µM, cast at 07:14), and GO32 (297 to 265 µM).

The profiles of fluorescence and turbidity displayed site-specific differences (Figure 2). Fluorescence and turbidity values at all stations tended to be fairly homogenous within the mixed layer. At all stations apart from GO12, surface fluorescence was close to 1.3 RFU, while at GO12 it was closer to 0.88 RFU. Fluorescence was generally most variable beneath the mixed layer, at depths between 25 and 40 m. Troughs in fluorescence in this range were noted at GO27, GO23, and at TF260. Turbidity profiles displayed similar trends in these depth ranges.

Temperatures throughout the water column at all stations decreased from roughly  $15^{\circ}$ C in the surface waters to  $7^{\circ}$ C at depth (see Figure 3). The temperature remained stable between  $14^{\circ}$ C and  $15^{\circ}$ C within the mixed layer. The depth of the thermocline varied between sites. The thermocline at stations GO12, GO32, and TF271 fell between 20 and 22 m, while stations GO23, GO24, and GO27 had thermocline depths of 26-27 m, and station TF260 exhibited the deepest thermocline at approximately 31 m. A bivariate fit shows some correlation (P=0.0306) between the thermocline depth and water column depth across all stations, with shallower stations tending to have larger mixed layers and deeper thermoclines.

The general trends in salinity were the same at all sites (Figure S3 in Supporting Information S1). In the surface waters, the salinity was roughly 7.4 and increased to 9–10 PSU by 80 m. A layer of intermediate salinity (25–60 m) was seen at Stations GO32, GO27, and TF260, but was not notable at the other stations. An oxycline appearing roughly between 75 and 90 m at all stations separates oxygenated surface waters from oxygen depleted bottom waters.

#### 3.2. Superoxide Concentrations With Depth

The distribution of superoxide through the water column followed a similar pattern at most sites (Figure 3). Concentrations were largely uniform through the mixed layer (0–20 m), with an emergent subsurface peak just below this mixed layer, after which concentrations decline to near or below surface values by a depth of 80 m. Superoxide in surface waters ranged between 1.6 and 7.6 nM. Superoxide in the first 5 m of the water column was visibly higher than the rest of the mixed layer in profiles at just three of the stations, TF260, TF271, and GO32.

TAENZER ET AL. 5 of 15

2169291, 2024, 10, Downloaded from https://agupubs.onlinelibrary.wiley.com/doi/10.1029/2024JC021438 by Mehigian State University, Wiley Online Library on [20/12/2024]. See the Terms and Conditions (https://onlinelibrary.wiley.com/terms-and-conditions) on Wiley Online Library for rules of use

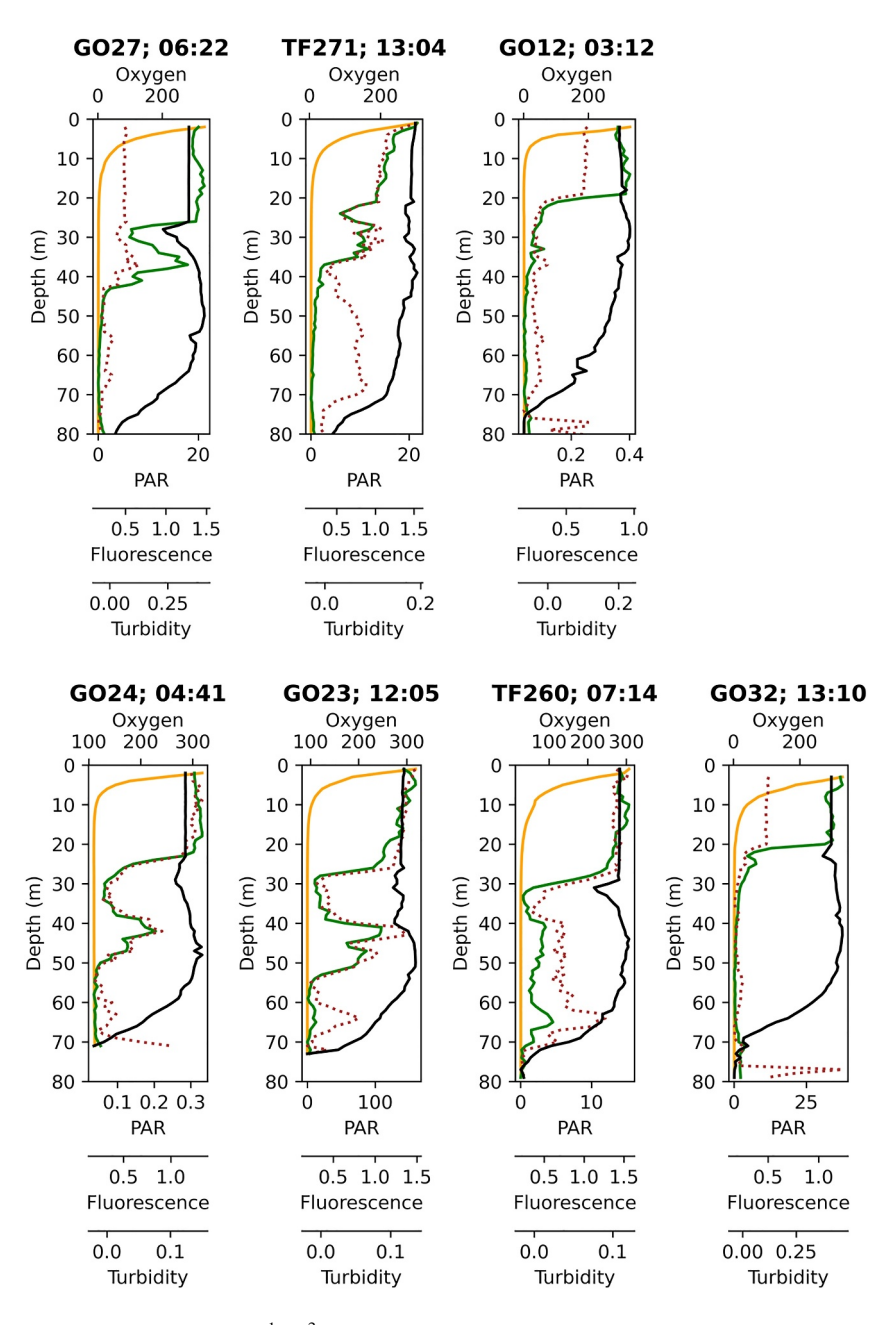


Figure 2. A comparison of PAR ( $\mu$ mol s<sup>-1</sup> m<sup>-2</sup>; solid yellow line), fluorescence ( $\mu$ g Chl/L; solid green line), turbidity (NTU; dashed red line), and oxygen ( $\mu$ M; solid black line) profiles across the seven sites studied.

Apart from these instances, surface concentrations of superoxide were not notably higher than in the rest of the mixed layer below 2 m.

Distinctive subsurface peaks of superoxide were observed to varying degrees in all casts at every station (Figure 3). The subsurface maxima consistently appeared at depths between 23 and 35 m. The highest concentrations reached at these depths varied between 2.0 nM at GO23, and 15.1 nM at TF260. In all instances, apart from one cast at GO23, the concentration of superoxide at the subsurface peak was the highest observed over the 80 m water column. In some cases, this constituted a 2 to 3-fold increase in concentration from the superoxide levels in the overlying mixed layer. The shape of the superoxide peaks was quite variable. The broadest superoxide increases were visible at GO12 and GO24. The smallest subsurface peaks in terms of concentration were seen at GO23 and GO32. The results of a one-way analysis of variance show that the subsurface concentrations of

TAENZER ET AL. 6 of 15

2169291, 2024, 10, Downloaded from https://agupubs.onlinelibrary.wiley.com/doi/10.1029/2024JC021438 by Michigan State University, Wiley Online Library

conditions) on Wiley Online Library for rules of use; OA articles are governed by the applicable Creat

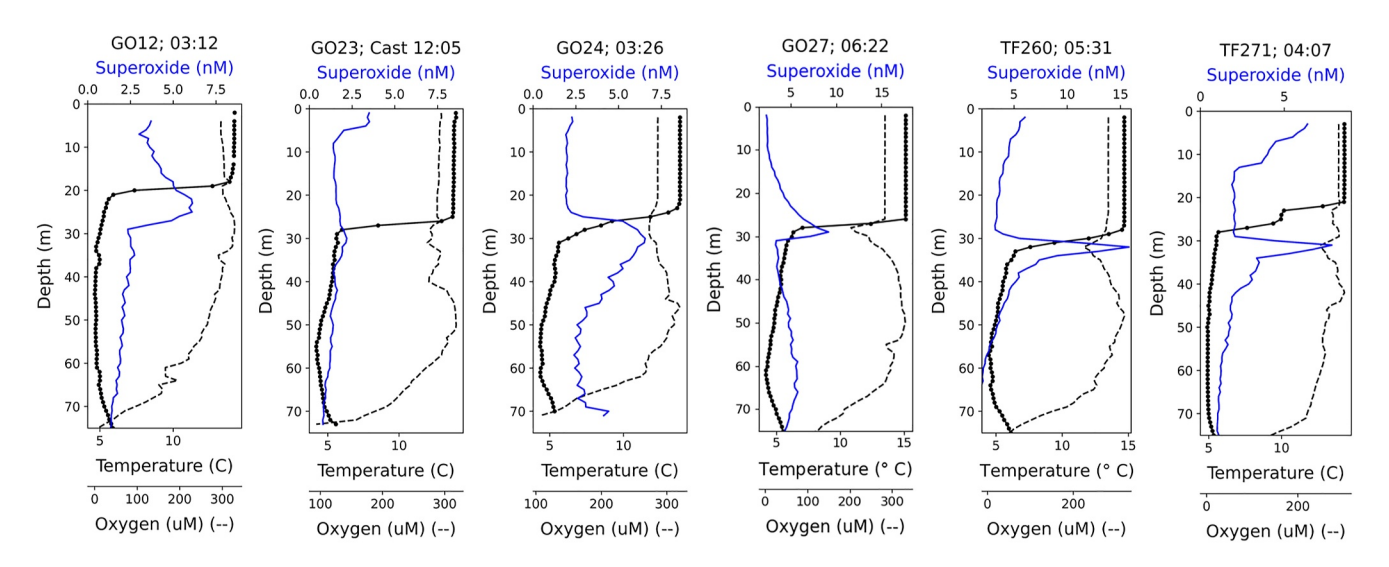


Figure 3. Superoxide depth profiles along thermocline and oxycline transitions.

superoxide were statistically different (P = 0.0342) between stations, with the highest concentrations measured at TF260.

In many of the casts local dips in oxygen also occur at a depth of 24 m (Figure 2). This oxygen concentration feature was most defined at casts at GO27 (dropping from 280 to 200  $\mu$ M), TF260 (280 to 216  $\mu$ M, cast at 07:14), and GO32 (297 to 265  $\mu$ M). At station TF260, where four oxygen profiles were measured throughout the day, the decrease in oxygen varied among profiles (see Figure S2 in Supporting Information S1). For instance, a more pronounced decline in oxygen was seen at 05:31 and 07:14 at Station TF260, than during profiles at 11:57 and 12:58.

# 3.3. Diel Superoxide Profiles

At some stations multiple profiles were collected throughout the day (TF260, TF271, GO23, and GO24). As seen in Figure 4 and Figure S2 in Supporting Information S1, superoxide concentrations and distributions varied over the course of the day. At station TF271 the highest concentrations of superoxide at the base of the mixed layer were observed at 13:04, while the early morning cast at 04:07 exhibited the most notable decline with depth from

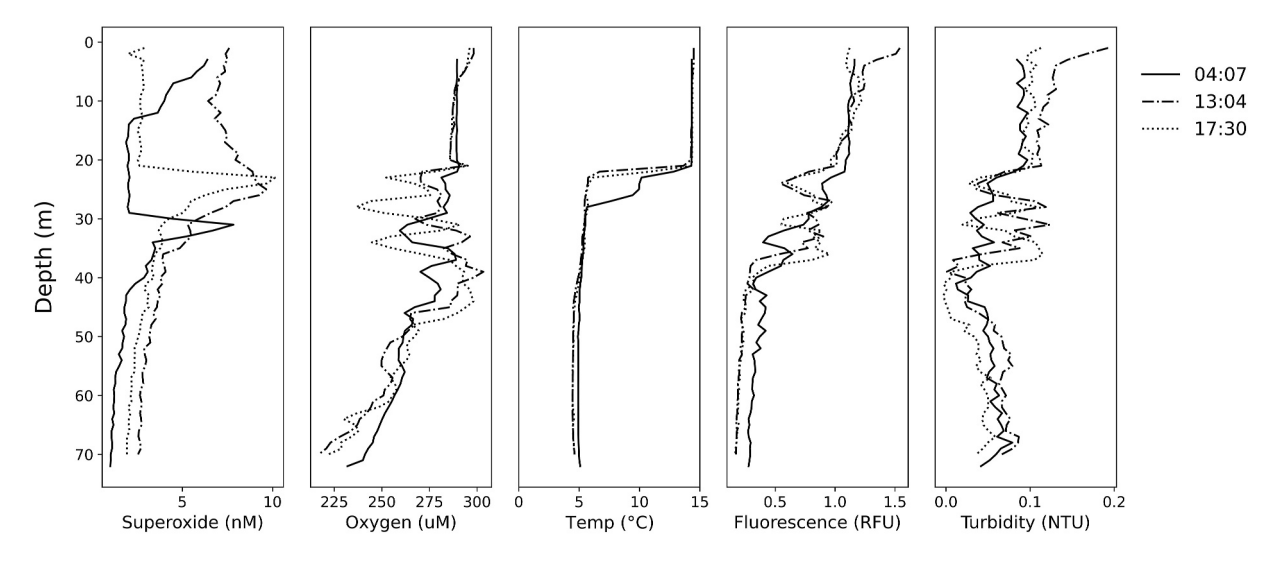


Figure 4. A comparison of superoxide, oxygen, temperature, fluorescence, and turbidity, as a function of time of day at Station TF271.

TAENZER ET AL. 7 of 15

3 m to the base of the euphotic zone. No significant correlations were found between surface superoxide concentrations and time of day or station.

The deeper thermocline at 04:07 was aligned with the deepest superoxide peak. However, time of day alone did not reveal any clear relationship with maximum subsurface superoxide concentrations. There were also notable variations in the dips and peaks in the oxygen profiles over time, as can be seen in the three profiles at TF271 from 04:07, 13:04 and 17:30 (see Figure 4). Turbidity and fluorescence patterns shifted in similar ways across the course of the day.

# 4. Discussion

# 4.1. Steady-State Superoxide in the Baltic Sea

We collected superoxide measurements during 15 casts over eight stations across light and dark cycles. Overall concentrations of superoxide measured here were largely higher than previously described in seawater (Figures 3 and 4). Earlier studies have reported concentrations up to 2,000 pM in sunlit surface waters, while estimates of superoxide in aphotic seawaters lie in the range of just a few picomolar (Hansard et al., 2010; Roe et al., 2016; Rose et al., 2008; Rusak et al., 2011; Schnur et al., 2024).

Seawater concentrations of superoxide are expected to vary with location, season, and climate, reflecting shifts in the strength of different production sources. In addition to these factors, one significant distinction that could account for the discrepancy in concentration magnitudes observed in our study compared to most previous work is the method of superoxide characterization. Previous estimates of superoxide concentrations have been made from extrapolations from decay rates (Hansard et al., 2010; Heller & Croot, 2010a; Rose et al., 2008; Rusak et al., 2011), or differences between particle-associated (unfiltered) and non-particle associated (filtered) waters collected from bottles (Roe et al., 2016; Sutherland, Grabb, et al., 2020). Therefore, any superoxide lost during initial decay, or from pathways other than particle associated production, is not taken into consideration, resulting in an underestimation of total concentrations. In this study, chemiluminescent measurements of unfiltered seawater were made directly in the environment, eliminating the need to account for decay rates. The one previous study conducted with SOLARIS highlighted similar concentrations to those here, of 7-16 nM off Western California (Taenzer et al., 2022). Similarly, work done with a diver operated in situ sensor in open ocean waters and coral reef environments (Diaz et al., 2016; Grabb et al., 2019) found similar shallow water (2-10 m) concentrations in the range of 2-8 nM, as seen in our Baltic Sea data. Together these studies suggest that in situ measurements are allowing us to capture total superoxide concentrations via a variety of pathways and sources (e.g., light-dependent and -independent; free and particle associated sources), thereby providing a more comprehensive picture of the superoxide landscape in the ocean. We note that chemiluminescent flow through systems, such as the one we have used here, could allow for bioluminescence of cells to be interested as MCLA chemiluminescence. However, we believe this to have had a negligible effect on our results, as the sampling wand of SOLARIS is outfitted with a filter tip (0.025 cm holes) which would have prevented a large portion of bioluminescent sources from entering the flow cell. Further, any exceptionally high data points (which were few and far between) were considered outliers and removed from any further analysis.

# 4.2. Water Column Distribution of Superoxide in the Baltic Sea

The most striking feature revealed in our data is the presence of a superoxide peak in the depth range of 23-35 m, which we hypothesize to originate from light-independent biological production. The smallest of these peaks was 2.0 nM at GO23 (13:01), while the highest peak reached 15.1 nM at TF260 (cast at 05:31 a.m.) (see Figure 3). A one-way ANOVA shows that stations are statistically different in their superoxide peaks indicating that local chemical and biological conditions play an important control on the balance between production and decay mechanisms (p = 0.0342). However, no simple relationships between superoxide maxima and depth, or proximity to land are evident. The maximum concentrations reached at the subsurface peaks do not display a clear relationship with time. At TF260, concentrations decline from 15.1 nM at the earliest morning cast done at 05:30 hr to 6.7 nM at 12:58, while the opposite trend emerges at station TF271 where an increase from 6.7 to 10.1 nM is seen between 04:07 and 17:31. This lack of clear diel pattern is perhaps not surprising as the observed maxima lie below the euphotic zone, which reached between 10 and 22 m across stations, and thus is not directly tied to a light-dependent source. Further corroborating this line of thought, the mean superoxide maxima and fluorescence values from each station also did not show a clear relationship (p = 0.0738). Fluorescence is

TAENZER ET AL. 8 of 15

commonly used as an indicator of phytoplankton abundance (Fragoso et al., 2021), and thus we would expect areas of photosynthetic activity by phytoplankton to align with higher fluorescence values. While extracellular superoxide production is common among phytoplankton, and axenic cultures (10<sup>3</sup>-10<sup>6</sup> cells mL<sup>-1</sup>) can produce superoxide in the range of 0.1 to tens of nanomolar (Diaz et al., 2018; Hansel & Diaz, 2021), presence and/or abundance of photosynthetic organisms do not appear as good predictors of superoxide concentrations in this study.

Light-independent biological processes are also a pathway for appreciable superoxide production in aphotic (and photic) marine systems (Diaz et al., 2013; Hansel et al., 2016; Kustka et al., 2005; Learman et al., 2011; Sutherland, Grabb, et al., 2020). The mechanisms by which heterotrophs produce ROS are less certain than for phytoplankton but may be linked to transmembrane NADPH oxidase (NOX) (Hajjar et al., 2017) or via soluble extracellular enzymes or reactive metabolites (Andeer et al., 2015; Diaz et al., 2019). Previous studies investigating particle-associated reactions have demonstrated significant production of superoxide to natural waters (Roe et al., 2016; Rose et al., 2008; Zhang et al., 2016). A microbial origin of the observed superoxide peak would suggest elevated activity in the 23 to 35 m depth range. Indeed, the regulation of microbial activity near the base of the euphotic zone is likely closely tied to patterns of primary productivity in the surface waters. The Baltic Sea is characterized by an unusual bloom pattern, with one large spring bloom of diatoms and flagellates, and a summer bloom dominated by nitrogen-fixing cyanobacteria (Legrand et al., 2015). A study done in the Northern Baltic Sea found that the highest percentage of labile dissolved organic carbon (DOC) (5%-9%) was found in the late summer and autumn (Hoikkala et al., 2015). Heterotrophic bacteria degrade DOC, with limitations on growth imposed by factors such as nutrient availability and temperature (Williams, 1995; Zweifel et al., 1995). As such, one might expect that the high quantities of labile DOC in the water column in autumn (when our study was conducted) would support enhanced microbial activity. This presumption is also supported by reports of a peak in heterotrophic bacterial biomass of 6.6–8.4 μmol C L<sup>-1</sup> after the late summer bloom in the Northern Baltic Sea (Hoikkala et al., 2012). Furthermore, our observations show that superoxide peaks emerge consistently below or at the base of the thermocline (see Figure 3), where sinking organic matter normally accumulates and the breakdown of thermal stratification in late September (Hoikkala et al., 2012) could lead to the injection of a fresh supply of labile DOC via water mixing stimulating growth.

Steady-state concentrations of superoxide in seawater are maintained as a balance between active production and decay mechanisms. Typical decay rate constants of superoxide in natural waters range between 0.002–0.016 s<sup>-1</sup> (Hansard et al., 2010). Assuming an average decay constant of 0.008 s<sup>-1</sup>, a production rate of 58 nM hr<sup>-1</sup> and 435 nM hr<sup>-1</sup> would be required to sustain our lowest and highest steady-state concentration at GO23 and TF260, respectively. To determine whether these rates are consistent with solely biological origins, we can compare these concentrations to previously reported rates of extracellular superoxide production by common microbes in the environment. Superoxide production rates for phytoplankton species range between 10<sup>-5</sup> and 10<sup>4</sup> amol cell<sup>-1</sup> h<sup>-1</sup> (Hansel & Diaz, 2021) while for heterotrophic microbes production has been reported to span from 0.1 to 3.7 amol cell<sup>-1</sup> h<sup>-1</sup> (Diaz et al., 2013; Sutherland et al., 2019). While cell abundance data were not recorded during our cruise, using a rough estimate of  $8 \times 10^6$  cell mL<sup>-1</sup> (directed by data from Wikner and Vikstrom (2023) as representative cell densities of the Baltic Sea) yield an estimated production rate of 7.3 and 54 amol cell<sup>-1</sup> h<sup>-1</sup> to cover the lowest and highest superoxide peaks, respectively. While these are higher than the production rates that have previously been found in lab-based studies of heterotrophs, superoxide production is known to be affected by several parameters that may be different in the environment than under lab conditions, including microbial interactions, nutrient availability, and cell density which shows an inverse relationship with superoxide production rate (Hansel et al., 2019).

Higher rates of light-independent extracellular superoxide production at depths of 25–35 m could also reflect a shift in microbial community structure. The absence of light, and rapid change in temperature from the overlying water column may provide an environmental niche allowing for the emergence of a distinct microbial community with different (co)-metabolisms. While the reasons for microbial extracellular superoxide production are not well known, the widespread occurrence of this peak at this depth suggests that it may provide some physiological advantage for cell growth, perhaps operating in the breakdown of DOM or nutrient acquisition (Hansel & Diaz, 2021). In addition, the observed distribution of superoxide could be in part accounted for by diel migration of phytoplankton or zooplankton. Previous observations of vertical dinoflagellate migration have been made at Gotland deep (Kowaleski, 2015) and the harmful algal bloom forming species, *Dinophysis acuminata*, have been

TAENZER ET AL. 9 of 15

noted to accumulate below the thermocline (Setälä et al., 2005), in the depths thar are particularly relevant to the superoxide peak we characterized here.

Beyond biological production, superoxide production in dark waters may occur through reactions with reduced. redox-active species. These include oxidation of Cu(I), Fe(II), and Mn(III) (within MnO<sub>2</sub>) by oxygen, or the reduction of Mn(IV) by H<sub>2</sub>O<sub>2</sub> (Morris et al., 2022). In particular, considerable work has looked at the role of Fe in the production and consumption of ROS (Fujii et al., 2010; Rose et al., 2005; Rose & Waite, 2002; Shaw et al., 2021). Oxygenation of dissolved inorganic Fe(II) may lead to the production of superoxide, with a wide range of reported oxidation rates (2.8–69 M<sup>-1</sup> s<sup>-1</sup>) depending on the organic or inorganic form of Fe and general seawater chemistry (Fujii et al., 2010; Gonzalez-Davila et al., 2005; Pham & Waite, 2008; Rush & Bielski, 1985; Santana-Casiano et al., 2006). Previous studies highlight a wide range of Fe(II) concentrations in the oxic upper water column (Breitbarth et al., 2009; Pohl & Fernández-Otero, 2012), but higher estimates of particulate Fe above the halocline of 31.4 nmol L<sup>-1</sup> (see Pohl & Hennigs et al., 2005) suggest that Fe(II) may have a role in superoxide cycling. Similarly, the presence of Mn in the oxic portion of the water column, as Mn(II) (14-50 nM), and particulate manganese (10-15 nM) (Neretin et al., 2003) suggests a potential role of Mn in superoxide formation. While the presence of redox-active trace metals allows for the possibility of superoxide generating reactions, why this would occur at substantially elevated rates in the depth range of 23-35 m remains an open question. As the water column is still fully oxygenated in this depth range, it doesn't fit the explanation of an interface environment where reduced species come in contact with oxygen, which has previously been noted to produce considerable pulses of ROS (Morris et al., 2022). Bacterial production of extracellular superoxide may oxidize Mn(II) to Mn(III, IV) oxides (Learman et al., 2011), and similarly has been proposed to facilitate microbial Fe acquisition under some environmental conditions (Rose, 2012), underlining the possibility that an overlap between microbial groups and metals could play a role in controlling superoxide levels in seawater.

The vertical trend in superoxide observed here in the Baltic Sea is similar to that reported in seawater east of New Zealand (Rusak et al., 2011), where a superoxide peak of 32.1 nM in unfiltered waters was found at approximately 40 m, and in the Costa Rica dome where a peak of above 150 pM was found (Rose et al., 2008). Together, these data begin to shift our understanding of the sources of superoxide in seawater away from photochemical production as the dominant source as has long been believed (Baxter & Carey, 1983; Micinski et al., 1993). In fact, in only about one-half (eight out of 15) of the water column superoxide profiles did we observe any decrease in superoxide concentrations from the first 2–5 m of the water column to the base of the euphotic zone (Figure 5). The highest near-surface concentrations we observed were at Station TF271 at 04:07, and at Station GO23 (10:08; 12:03; and 13:01). In all other profiles, concentrations within the euphotic zone do not appear to reflect elevated surface production. It is important to note that due to the positioning of SOLARIS on the CTD, we don't have data on superoxide for the first 2 m of the water column where photochemical production is expected to be most significant. Nevertheless, the lack of trend from 2 m to deeper suggests that photochemical production was a minimal source below 2 m at the time that we sampled most stations.

# 4.3. Oxygen Loss and Superoxide Production

At several stations (e.g., GO27, TF260, and GO32), the subsurface peak in superoxide is mirrored by a clear dip in oxygen (Figure 5). Local oxygen minima located at the base of the thermocline have previously been observed in the later summer in the northern Baltic Sea (Raateoja et al., 2010). This feature has been explained as a hotspot of organic matter decomposition driven by a slowing in the sinking speed of particles around 20 meters due to a temperature driven density gradient (Horppila et al., 2000). Oxygen use at this depth has on average been attributed to microbial decomposition (~80%) and mesozooplankton respiration (~20%) (Raateoja et al., 2010). As in previous studies, we interpret the dip in oxygen at the base of the thermocline to relfect an increased rate of oxygen consumption via microbial decomposition. The first derivative of oxygen with depth, seen as an example for Station TF260 (chosen due to the multiple casts done at this station) in Figure 6, shows the relative change in oxygen consumption at 1-m intervals. The superoxide standing stock within the subsurface peak (nmoles m<sup>-2</sup>) was estimated by integrating the peak area. The superoxide concentration directly before the onset of the peak (above the peak) was considered as the baseline. Peak area between these intervals was calculated by trapezoidal integration. A similar technique was used to quantify the integrated loss of oxygen represented in the corresponding oxygen profile at these same depth intervals.

TAENZER ET AL. 10 of 15



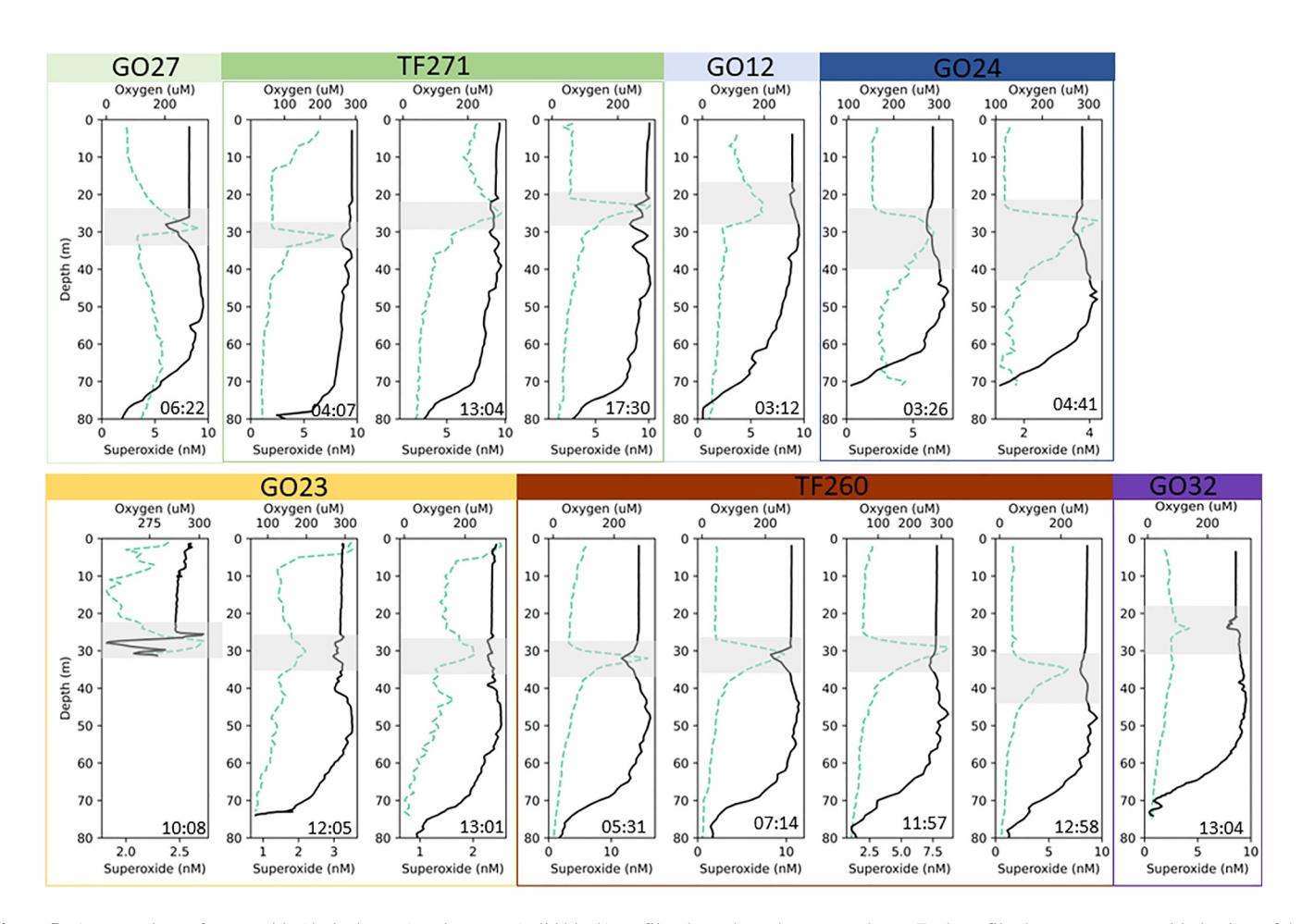


Figure 5. A comparison of superoxide (dashed green) and oxygen (solid black) profiles throughout the water column. Each profile shows a new cast with the time of the cast in the lower right portion of each plot. The gray shaded region highlights the position of the subsurface superoxide peak.

As indicated by the overlap between the large negative excursion and the maxima in the superoxide profile, superoxide peaks consistently emerge in defined areas in the upper water column exhibiting high relative rates of oxygen drawdown. Rates of oxygen decline lower in the water column and then increase again in the vicinity of the sharp chemocline, until oxygen eventually drops to near zero by 80 m.

Prokaryotic respiration in the Baltic Sea varies with location, depth, and season, among other factors (Kuprinen, 1987; Rychert et al., 2015; Spilling et al., 2019). An average respiration rate of 2.9 ( $\pm$ 2.4)  $\mu$ mol L<sup>-1</sup> d<sup>-1</sup> (Wikner & Vikstrom, 2023) for the Baltic Sea is notably lower than our estimated superoxide production rate, even for our lowest superoxide peak which converts to 4.8  $\mu$ mol L<sup>-1</sup> d<sup>-1</sup>. The mismatch between these rates does not refute that heterotrophs are producing the majority of extracellular superoxide, but rather suggests that extracellular superoxide is a co-metabolic rather than a direct metabolic product.

The considerable steady-state concentrations of superoxide observed in the Baltic Sea may amplify the already high rates of oxygen loss in this environment. The different fates of superoxide in seawater have unique implications for the marine oxygen budget. If superoxide is reduced to hydrogen peroxide, rather than re-oxidized, a net loss of oxygen ensues. Integration of the superoxide peak over the 29–37 m depth range for the 05:31 cast at TF260 yields an estimated superoxide concentration of  $50 \, \mu \text{mol m}^{-2}$ . Adopting previously established bounds for the net oxygen reduction from superoxide production of 14%–53% (Sutherland et al., 2019), we estimate that within this depth range, the flux of superoxide production may lead to the loss of 7–27  $\mu \text{mol m}^{-2}$  of oxygen. Interestingly, there is a visible drop in oxygen that mirrors the superoxide peak at this time. Integrating the amount of oxygen lost in this depth interval indicates  $218 \, \mu \text{mol m}^{-2}$  have been consumed. Thus, for this particular profile the flux of superoxide could account for somewhere between 3% and 12% of the oxygen loss. While a decrease in oxygen at the same depth as elevated superoxide levels was a common feature, it was not always notable, and at

TAENZER ET AL. 11 of 15

21699291, 2024, 10, Downl

from https://agupubs.onlinelibrary.wiley.com/doi/10.1029/2024JC021438 by Michigan State University, Wiley Online Library on [20/12/2024]. See:

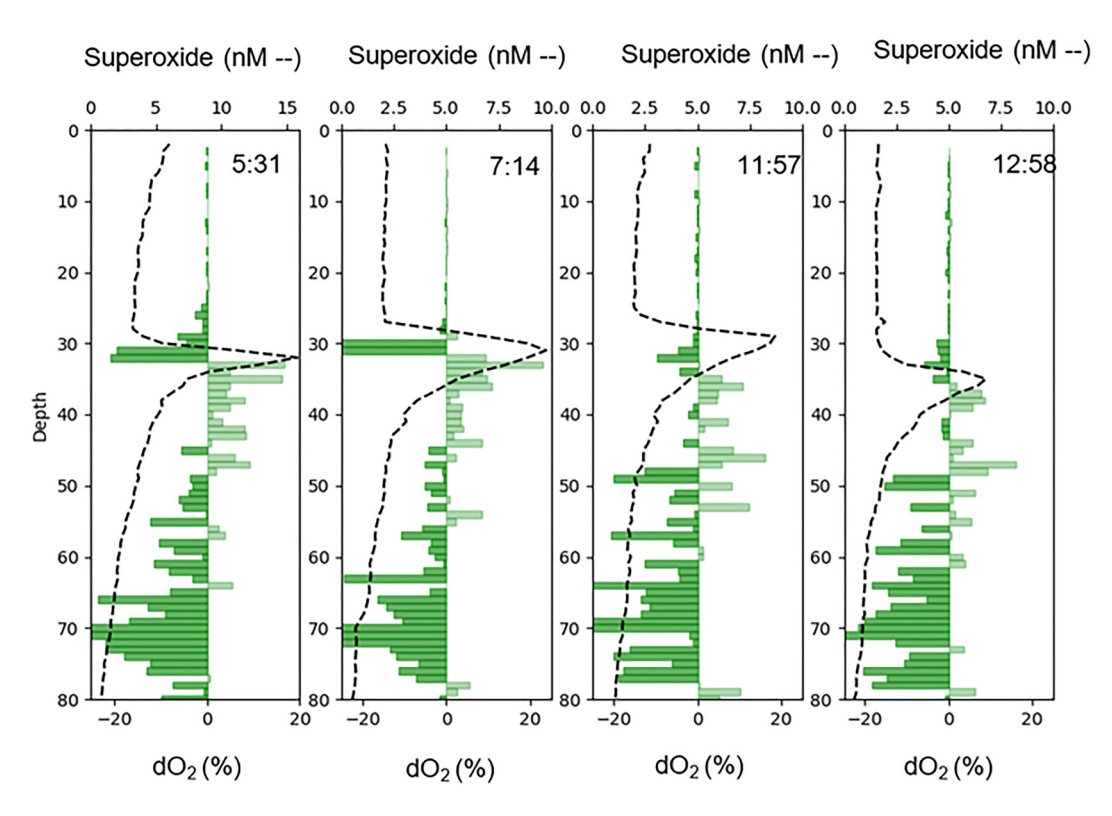


**Figure 6.** An illustration of superoxide profiles (in dashed line) imposed on the first derivative of oxygen (green bars) with depth during each cast at TF260.

times the two features appeared slightly offset. For instance, in the 03:26 a.m. cast at GO24 there is a peak in integrated superoxide of  $58 \mu mol \ m^{-2}$  between 25 and 40 m depth, whereas the integrated decrease in oxygen of 90  $\mu mol \ m^{-2}$  occurs further up in the water column between 22 and 34 m. Thus, while the flux of ROS may be an important component influencing the oxygen budget of the Baltic Sea, a clear quantitative relationship between two coinciding features was not necessarily universal and thus requires further investigation.

# 5. Conclusions

Our observations of superoxide play into an emerging understanding of the biogeochemical intricacy of the Baltic Sea. While previous work has pointed to the apparently ubiquitous generation of ROS in seawater, this study demonstrates the presence of superoxide at concentrations in dark subsurface waters that have rarely been captured. The concentrations of superoxide that we observed in the water column of the Baltic Sea will affect the redox chemistry of metals (e.g., Cu, Fe, Mn) and carbon, with important implications for solubility, biological availability, and toxicity (Sunda & Huntsman, 1998). Furthermore, the flux of superoxide has been previously implicated in net oxygen loss (Sutherland et al., 2019), and we indicate that it may be one component driving local oxygen dips at the depths of the superoxide maxima.

Our findings suggest that the concentrations and distributions of superoxide in the Baltic Sea in the late summer to early Fall are not dominated by photochemical production, but rather by sustained and elevated steady-state biological production in waters directly below the thermocline. A shift from considering abiotic production as the dominant production pathway under all conditions to recognizing the importance of biotic sources both seasonally and locally emphasizes the gaps in our understanding of the controls of superoxide dynamics in the ocean. Future research should specifically target the link between microbial respiration/activity and superoxide production, and the subsequent impact of superoxide on carbon and nutrient cycling. This work also inspires inquiries into further ocean basins to determine whether subsurface superoxide has been an overlooked aspect to redox biogeochemistry more broadly.

TAENZER ET AL. 12 of 15



# Journal of Geophysical Research: Oceans

10.1029/2024JC021438

# **Data Availability Statement**

CTD and superoxide data used in this study can be found at Biological and Chemical Oceanography Data Management Office (BCO-DMO) project number 929159 (https://www.bco-dmo.org/award/929159) Taenzer and Hansel (2024a, 2024b).

#### Acknowledgments

We thank the crew and captain of the RV Elisabeth Mann Borgese for their support during the EMB276 cruise. This work was funded by the National Science Foundation Chemical Oceanography program Grant OCE-1924236 to CMH and SDW and OCE-1923218 to DSH.

#### References

- Aguirre, J., Rios-Momberg, M., Hewitt, D., & Hansberg, W. (2005). Reactive oxygen species and development in microbial eukaryotes. *Trends in Microbiology*, 13(3), 111–118. https://doi.org/10.1016/j.tim.2005.01.007
- Andeer, P. F., Learman, D. R., McIlvin, M., Dunn, J. A., & Hansel, C. M. (2015). Extracellular haem peroxidases mediate Mn(II) oxidation in a marine Roseobacter bacterium via superoxide production. Environmental Microbiology, 17(10), 3925–3936. https://doi.org/10.1111/1462-2920.12893
- Archibald, F. S., & Fridovich, I. (1982). The scavenging of superoxide radical by manganous complexes: In vitro. Archives of Biochemistry and Biophysics, 214(2), 452–463. https://doi.org/10.1016/0003-9861(82)90049-2
- Baxter, R. M., & Carey, J. H. (1983). Evidence for photochemical generation of superoxide ion in humic waters. *Nature*, 306(5943), 575–576. https://doi.org/10.1038/306575a0
- Breitbarth, E., Gelting, J., Walve, J., Hoffmann, L. J., Turner, D. R., Hassellöv, M., & Ingri, J. (2009). Dissolved iron (II) in the Baltic Sea surface water and implications for cyanobacterial bloom development. *Biogeosciences*, 6(11), 2397–2420. https://doi.org/10.5194/bg-6-2397-2009
- Buetler, T. M., Krauskopf, A., & Ruegg, U. T. (2004). Role of superoxide as a signaling molecule. *Physiology*, 19(3), 120–123. https://doi.org/10.1152/nips.01514.2003
- Carstensen, J., Andersen, J. H., Gustafsson, B. G., & Conley, D. J. (2014). Deoxygenation of the Baltic Sea during the last century. Proceedings of the National Academy of Sciences, 111(15), 5628–5633. https://doi.org/10.1073/pnas.1323156111
- Dellwig, O., Leipe, T., März, C., Glockzin, M., Pollehne, F., Schnetger, B., et al. (2010). A new particulate Mn–Fe–P-shuttle at the redoxcline of anoxic basins. *Geochimica et Cosmochimica Acta*, 74(24), 7100–7115. https://doi.org/10.1016/j.gca.2010.09.017
- Diaz, J. M., Hansel, C. M., Apprill, A., Brighi, C., Zhang, T., Weber, L., et al. (2016). Species-specific control of external superoxide levels by the coral holobiont during a natural bleaching event. *Nature Communications*, 7(1), 13801. https://doi.org/10.1038/ncomms13801
- Diaz, J. M., Hansel, C. M., Voelker, B. M., Mendes, C. M., Andeer, P. F., & Zhang, T. (2013). Widespread production of extracellular superoxide by heterotrophic bacteria. *Science*, 340(6137), 1223–1226. https://doi.org/10.1126/science.1237331
- Diaz, J. M., Plummer, S., Hansel, C. M., Andeer, P. F., Saito, M. A., & McIlvin, M. R. (2019). NADPH-dependent extracellular superoxide production is vital to photophysiology in the marine diatom *Thalassiosira oceanica*. *Proceedings of the National Academy of Sciences*, 116(33),
- 16448–16453. https://doi.org/10.1073/pnas.1821233116
  Diaz, J. M., Plummer, S., Tomas, C., & de Souza, C. A. (2018). Production of extracellular superoxide and hydrogen peroxide by five marine species of harmful bloom-forming algae. *Journal of Plankton Research*, 40(6), 667–677. https://doi.org/10.1093/plankt/fby043
- Fragoso, G. M., Johnsen, G., Chauton, M. S., Cottier, F., & Ellingsen, I. (2021). Phytoplankton community succession and dynamics using optical approaches. Continental Shelf Research, 213, 104322. https://doi.org/10.1016/j.csr.2020.104322
- Fujii, M., Rose, A. L., Waite, T. D., & Omura, T. (2010). Oxygen and superoxide-mediated redox kinetics of iron complexed by humic substances in coastal seawater. *Environmental Science and Technology*, 44(24), 9337–9342. https://doi.org/10.1021/es102583c
- Garg, S., Rose, A. L., & Waite, T. D. (2011). Photochemical production of superoxide and hydrogen peroxide from natural organic matter. Geochimica et Cosmochimica Acta, 75(15), 4310–4320. https://doi.org/10.1016/j.gca.2011.05.014
- Gonzalez-Davila, M., Santana-Casiano, J. M., & Millero, F. J. (2005). Oxidation of iron (II) nanomolar with H<sub>2</sub>O<sub>2</sub> in seawater. *Geochimica et Cosmochimica Acta*, 69(1), 83–93. https://doi.org/10.1016/j.gca.2004.05.043
- Grabb, K. C., Kapit, J., Wankel, S. D., Manganini, K., Apprill, A., Armenteros, M., & Hansel, C. M. (2019). Development of a handheld submersible chemiluminescent sensor: Quantification of superoxide at coral surfaces. *Environmental Science and Technology*, 53(23), 13850–13858. https://doi.org/10.1021/acs.est.9b04022
- K. Grasshoff, K. Kremling, & M. Ehrhardt (Eds.) (1999). Methods of seawater analysis. Wiley. https://doi.org/10.1002/9783527613984
- Hajjar, C., Cherrier, M. V., Mirandela, G. D., Petit-Hartlein, I., Stasia, M. J., Fontecilla-Camps, J. C., et al. (2017). The NOX family of proteins is also present in bacteria. mBio, 8(6). https://doi.org/10.1128/mbio.01487-17
- Hansard, S. P., Easter, H. D., & Voelker, B. M. (2011). Rapid reaction of nanomolar Mn(II) with superoxide radical in seawater and simulated freshwater. *Environmental Science and Technology*, 45(7), 2811–2817. https://doi.org/10.1021/es104014s
- Hansard, S. P., Vermilyea, A. W., & Voelker, B. M. (2010). Measurements of superoxide radical concentration and decay kinetics in the Gulf of Alaska. *Deep Sea Research Part I: Oceanographic Research Papers*, 57(9), 1111–1119. https://doi.org/10.1016/j.dsr.2010.05.007
- Hansel, C. M., Buchwald, C., Diaz, J. M., Ossolinski, J. E., Dyhrman, S. T., Mooy, B. A. S. V., & Polyviou, D. (2016). Dynamics of extracellular superoxide production by *Trichodesmium* colonies from the Sargasso Sea. *Limnology & Oceanography*, 61(4), 1188–1200. https://doi.org/10.1002/no.1006/6
- Hansel, C. M., & Diaz, J. M. (2021). Production of extracellular reactive oxygen species by marine biota. *Annual Review of Marine Science*, 13(1), 177–200. https://doi.org/10.1146/annurev-marine-041320-102550
- Hansel, C. M., Diaz, J. M., & Plummer, S. (2019). Tight regulation of extracellular superoxide points to its vital role in the physiology of the globally relevant *Roseobacter* clade. *mBio*, 10(2). https://doi.org/10.1128/mbio.02668-18
- HELCOM. (2017). HELCOM COMBINE manual. Retrieved from https://helcom.fi/actionareas/monitoringandassessment/monitoringguidelines/combinemanual/
- Heller, M. I., & Croot, P. L. (2010a). Kinetics of superoxide reactions with dissolved organic matter in tropical Atlantic surface waters near Cape Verde (Tenatso). *Journal of Geophysical Research*, 115(C12). https://doi.org/10.1029/2009jc006021
- Heller, M. I., & Croot, P. L. (2010b). Superoxide decay kinetics in the southern ocean. *Environmental Science and Technology*, 44(1), 191–196. https://doi.org/10.1021/es901766r
- Heller, M. I., & Croot, P. L. (2010c). Application of a superoxide (O<sub>2</sub><sup>-</sup>) thermal source (SOTS-1) for the determination and calibration of O<sub>2</sub><sup>-</sup> fluxes in seawater. *Analytica Chimica Acta*, 667(1–2), 1–13. https://doi.org/10.1016/j.aca.2010.03.054
- Hermans, M., Lenstra, W. K., Hidalgo-Martinez, S., van Helmond, N. A. G. M., Witbaard, R., Meysman, F. J., et al. (2019). Abundance and biogeochemical impact of cable bacteria in Baltic Sea sediments. *Environmental Science and Technology*, 53(13), 7494–7503. https://doi.org/10.1021/acs.est.9b01665

TAENZER ET AL. 13 of 15

- Hoikkala, L., Kortelainen, P., Soinne, H., & Kuosa, H. (2015). Dissolved organic matter in the Baltic Sea. *Journal of Marine Systems*, 142, 47–61. https://doi.org/10.1016/j.jmarsys.2014.10.005
- Hoikkala, L., Lahtinen, T., Perttilä, M., & Lignell, R. (2012). Seasonal dynamics of dissolved organic matter on a coastal salinity gradient in the northern Baltic Sea. Continental Shelf Research, 45, 1–14. https://doi.org/10.1016/j.csr.2012.04.008
- Horppila, J., Malinen, T., Nurminen, L., Tallberg, P., & Vinni, M. (2000). A metalimnetic oxygen minimum indirectly contributing to the low biomass of cladocerans in Lake Hiidenvesi - A diurnal study on the refuge effect. *Hydrobiologia*, 436(1/3), 81–90. https://doi.org/10.1023/A: 1026594006856
- Kowalewski, M. (2015). The flow of nitrogen into the euphotic zone of the Baltic proper as a result of the vertical migration of phytoplankton: An analysis of the long-term observations and ecohydrodynamic model simulation. *Journal of Marine Systems*, 145, 53–68. https://doi.org/10.1016/j.jmarsys.2015.01.003
- Kuprinen, J. (1987). Production and respiration of overall plankton and ultraplankton communities at the entrance to the Gulf of Finland in the Baltic Sea. *Marine Biology*, 93(4), 591–607. https://doi.org/10.1007/bf00392797
- Kustka, A. B., Shaked, Y., Milligan, A. J., King, D. W., & Morel, F. M. M. (2005). Extracellular production of superoxide by marine diatoms: Contrasting effects on iron redox chemistry and bioavailability. *Limnology & Oceanography*, 50(4), 1172–1180. https://doi.org/10.4319/lo. 2005.50.4.1172
- Laima, M. J. C., Matthiesen, H., Christansen, C., Lund-Hansen, L. C., & Emeis, K. C. (2001). Dynamics of P, Fe, and Mn along a depth gradient in the SW Baltic Sea. Boreal Environment Research. 6, 317–333.
- Lamb, C., & Dixon, R. A. (1997). The oxidative burst in plant disease resistance. Annual Review of Plant Physiology and Plant Molecular Biology, 48(1), 251–275. https://doi.org/10.1146/annurev.arplant.48.1.251
- Learman, D. R., Voelker, B. M., Madden, A. S., & Hansel, C. M. (2013). Constraints on superoxide mediated formation of manganese oxides. Frontiers in Microbiology, 4, 262. https://doi.org/10.3389/fmicb.2013.00262
- Learman, D. R., Voelker, B. M., Vazquez-Rodriguez, A. I., & Hansel, C. M. (2011). Formation of manganese oxides by bacterially generated superoxide. *Nature Geoscience*, 4(2), 95–98. https://doi.org/10.1038/ngeo1055
- Legrand, C., Fridolfsson, E., Bertos-Fortis, M., Lindehoff, E., Larsson, P., Pinhassi, J., & Andersson, A. (2015). Interannual variability of phyto-bacterioplankton biomass and production in coastal and offshore waters of the Baltic Sea. *Ambio*, 44(S3), 427–438. https://doi.org/10.1007/s13280-015-0662-8
- Li, H.-P., Daniel, B., Creeley, D., Grandbois, R., Zhang, S., Xu, C., et al. (2014). Superoxide production by a manganese-oxidizing bacterium facilitates iodide oxidation. *Applied and Environmental Microbiology*, 80(9), 2693–2699. https://doi.org/10.1128/AEM.00400-14
- Luther, G. W. (2023). Review on the physical chemistry of iodine transformations in the oceans. Frontiers in Marine Science, 10, 1085618. https://doi.org/10.3389/fmars.2023.1085618
- Matthäus, W., & Franck, H. (1992). Characteristics of major Baltic inflows—A statistical analysis. Continental Shelf Research, 12(12), 1375–1400. https://doi.org/10.1016/0278-4343(92)90060-W
- Micinski, E., Ball, L. A., & Zafiriou, O. C. (1993). Photochemical oxygen activation: Superoxide radical detection and production rates in the eastern Caribbean. *Journal of Geophysical Research*, 98(C2), 2299–2306. https://doi.org/10.1029/92jc02766
- Morris, J. J., Rose, A. L., & Lu, Z. (2022). Reactive oxygen species in the world ocean and their impacts on marine ecosystems. *Redox Biology*, 52, 102285. https://doi.org/10.1016/j.redox.2022.102285
- Neretin, L. N., Pohl, C., Jost, G., Leipe, T., & Pollehne, F. (2003). Manganese cycling in the Gotland deep, Baltic Sea. *Marine Chemistry*, 82(3–4), 125–143. https://doi.org/10.1016/S0304-4203(03)00048-3
- Ojaveer, H., Jaanus, A., MacKenzie, B. R., Martin, G., Olenin, S., Radziejewska, T., et al. (2010). Status of biodiversity in the Baltic Sea. *PLoS One*, 5(9), e12467. https://doi.org/10.1371/journal.pone.0012467
- Osburn, C. L., & Stedmon, C. A. (2011). Linking the chemical and optical properties of dissolved organic matter in the Baltic–North Sea transition zone to differentiate three allochthonous inputs. *Marine Chemistry*, 126(1-4), 281–294. https://doi.org/10.1016/j.marchem.2011.06.007
- Petasne, R. G., & Zika, R. G. (1987). Fate of superoxide in Coastal Sea Water. *Nature*, 325(6104), 516–518. https://doi.org/10.1038/325516a0 Pham, A. N., & Waite, T. D. (2008). Modeling the kinetics of Fe(II) oxidation in the presence of citrate and salicylate in aqueous solutions at pH 6.0-.08 and 25°C. *The Journal of Physical Chemistry A*, 112(24), 5395–5405. https://doi.org/10.1021/jp801126p
- Pohl, C., & Fernández-Otero, E. (2012). Iron distribution and speciation in oxic and anoxic waters of the Baltic Sea. *Marine Chemistry*, 145–147, 1–15. https://doi.org/10.1016/j.marchem.2012.09.001
- Pohl, C., & Hennings, U. (2005). The coupling of long-term trace metal trends to internal trace metal fluxes at the oxic-anoxic interface in the Gotland Basin (57 degrees 19, 200 N; 20 degrees 03,000 E) Baltic Sea. *Journal of Marine Systems*, 56(1–2), 207–225. https://doi.org/10.1016/j.imarsys.2004.10.001
- Powers, L. C., & Miller, W. L. (2014). Blending remote sensing data products to estimate photochemical production of hydrogen peroxide and superoxide in the surface ocean. Environmental Sciences: Processes & Impacts, 16(4), 792–806. https://doi.org/10.1039/c3em00617d
- Raateoja, M., Kuosa, H., Flinkman, J., Pääkkönen, J.-P., & Perttilä, M. (2010). Late summer metalimnetic oxygen minimum zone in the northern Baltic Sea. *Journal of Marine Systems*, 80(1–2), 1–7. https://doi.org/10.1016/j.jmarsys.2009.06.005
- Roe, K. L., & Barbeau, K. A. (2014). Uptake mechanisms for inorganic iron and ferric citrate in *Trichodesmium erythraeum* IMS101. *Metallomics*, 6(11), 2042–2051. https://doi.org/10.1039/c4mt00026a
- Roe, K. L., Schneider, R. J., Hansel, C. M., & Voelker, B. M. (2016). Measurement of dark, particle-generated superoxide and hydrogen peroxide production and decay in the subtropical and temperate North Pacific Ocean. *Deep Sea Research Part I: Oceanographic Research Papers*, 107, 59–69. https://doi.org/10.1016/j.dsr.2015.10.012
- Rose, A. L. (2012). The influence of extracellular superoxide on iron redox chemistry and bioavailability to aquatic microorganisms. Frontiers in Microbiology, 3, 124. https://doi.org/10.3389/fmicb.2012.00124
- Rose, A. L., Salmon, T. P., Lukondeh, T., Neilan, B. A., & Waite, T. D. (2005). Use of superoxide as an electron shuttle for iron acquisition by the marine cyanobacterium *Lyngbya majuscula*. *Environmental Science and Technology*, 39(10), 3708–3715. https://doi.org/10.1021/es048766c
- Rose, A. L., & Waite, T. D. (2002). Kinetic model for Fe(II) oxidation in seawater in the absence and presence of natural organic matter. *Environmental Science and Technology*, 36(3), 433–444. https://doi.org/10.1021/es0109242
- Rose, A. L., Webb, E. A., Waite, T. D., & Moffett, J. W. (2008). Measurement and implications of nonphotochemically generated superoxide in the equatorial Pacific Ocean. *Environmental Science and Technology*, 42(7), 2387–2393. https://doi.org/10.1021/es7024609
- Rusak, S. A., Peake, B. M., Richard, L. E., Nodder, S. D., & Cooper, W. J. (2011). Distributions of hydrogen peroxide and superoxide in seawater east of New Zealand. *Marine Chemistry*, 127(1–4), 155–169. https://doi.org/10.1016/j.marchem.2011.08.005
- Rush, J. D., & Bielski, B. H. J. (1985). Pulse radiolytic studies of the reaction of perhydroxyl/superoxide O<sub>2</sub>- with iron(II)/iron(III) ions. The reactivity of HO<sub>2</sub>/O<sub>2</sub>- with ferric ions and its implication on the occurrence of the Haber-Weiss reaction. *The Journal of Physical Chemistry*, 89(23), 5062–5066. https://doi.org/10.1021/j100269a035

TAENZER ET AL. 14 of 15

- Rychert, K., Wielgat-Rychert, M., Wol oszynek, M., & Sojda, G. (2015). Pelagic respiration in the coastal zone of the southern Baltic Sea. *Ecohydrology and Hydrobiology*, 15(4), 215–219. https://doi.org/10.1016/j.ecohyd.2015.06.001
- Santana-Casiano, J., González-Dávila, M., & Millero, F. (2006). The role of Fe(II) species on the oxidation of Fe(II) in natural waters in the presence of O<sub>2</sub>- and H<sub>2</sub>O<sub>2</sub>. Marine Chemistry, 99(1-4), 70-82. https://doi.org/10.1016/j.marchem.2005.03.010
- Schnur, A. A., Sutherland, K. M., Hansel, C. M., & Hardisty, D. S. (2024). Rates and pathways of iodine speciation transformations at the Bermuda Atlantic Time Series. Frontiers in Marine Science, 10, 1272870. https://doi.org/10.3389/fmars.2023.1272870
- Schulz-Vogt, H. N., Pollehne, F., Jürgens, K., Arz, H. W., Beier, S., Bahlo, R., et al. (2019). Effect of large magnetotactic bacteria with polyphosphate inclusions on the phosphate profile of the suboxic zone in the Black Sea. *The ISME Journal*, 13(5), 1198–1208. https://doi.org/10.1038/s41396-018-0315-6
- Setälä, O., Autio, R., Kuosa, H., Rintala, J., & Ylöstalo, P. (2005). Survival and photosynthetic activity of different Dinophysis acuminata populations in the northern Baltic Sea. *Harmful Algae*, 4(2), 337–350. https://doi.org/10.1016/j.hal.2004.06.017
- Shaked, Y., & Armoza-Zvuloni, R. (2013). Dynamics of hydrogen peroxide in a coral reef: Sources and sinks. *Journal of Geophysical Research: Biogeosciences*, 118(4), 1793–1801. https://doi.org/10.1002/2013jg002483
- Shaw, T. J., Luther, G. W., Rosas, R., Oldham, V. E., Coffey, N. R., Ferry, J. L., et al. (2021). Fe-catalyzed sulfide oxidation in hydrothermal plumes is a source of reactive oxygen species to the ocean. *Proceedings of the National Academy of Sciences*, 118(40), e2026654118. https://doi.org/10.1073/pnas.2026654118
- Spilling, K., Fuentes-Lema, A., Quemaliños, D., Klais, R., & Sobrino, C. (2019). Primary production, carbon release, and respiration during spring bloom in the Baltic Sea. *Limnology & Oceanography*, 64(4), 1779–1789. https://doi.org/10.1002/ino.11150
- Strady, E., Pohl, C., Yakushev, E. v., Krüger, S., & Hennings, U. (2008). PUMP–CTD-System for trace metal sampling with a high vertical resolution. A test in the Gotland Basin, Baltic Sea. Chemosphere, 70(7), 1309–1319. https://doi.org/10.1016/j.chemosphere.2007.07.051
- Sunda, W. G., & Huntsman, S. A. (1998). Processes regulating cellular metal accumulation and physiological effects: Phytoplankton as model systems. Science of the Total Environment, 219(2–3), 165–181. https://doi.org/10.1016/s0048-9697(98)00226-5
- Sutherland, K. M., Coe, A., Gast, R. J., Plummer, S., Suffridge, C. P., Diaz, J. M., et al. (2019). Extracellular superoxide production by key microbes in the global ocean. *Limnology & Oceanography*, 64(6), 2679–2693. https://doi.org/10.1002/lno.11247
- Sutherland, K. M., Grabb, K. C., Karolewski, J. S., Plummer, S., Farfan, G. A., Wankel, S. D., et al. (2020). Spatial heterogeneity in particle-associated, light-independent superoxide production within productive coastal waters. *Journal of Geophysical Research: Oceans*, 125(10), e2020JC016747. https://doi.org/10.1029/2020jc016747
- Sutherland, K. M., Wankel, S. D., & Hansel, C. M. (2020). Dark biological superoxide production as a significant flux and sink of marine dissolved oxygen. Proceedings of the National Academy of Sciences, 117(7), 3433–3439. https://doi.org/10.1073/pnas.1912313117
- Taenzer, L., Grabb, K., Kapit, J., Pardis, W., Wankel, S. D., & Hansel, C. M. (2022). Development of a deep-sea submersible chemiluminescent analyzer for sensing short-lived reactive chemicals. Sensors, 22(5), 1709. https://doi.org/10.3390/s22051709
- Taenzer, L., & Hansel, C. (2024a). SOLARIS superoxide and standard CTD profiles from the EMB276 cruise on R/V Elisabeth Mann Borgese in the Baltic Sea from September 20-27, 2021 [Dataset]. Biological and Chemical Oceanography Data Management Office (BCO-DMO). (Version 1) Version Date 2024-08-06. https://www.bco-dmo.org/award/929159
- Taenzer, L., & Hansel, C. (2024b). Pump CTD profiles from the EMB276 cruise on R/V Elisabeth Mann Borgese in the Baltic Sea from September 20-27, 2021 [Dataset]. Biological and Chemical Oceanography Data Management Office (BCO-DMO). (Version 1) Version Date 2024-08-06. https://demo.bco-dmo.org/award/929159
- Terzić, E., Zabłocka, M., Loginova, A. N., Borzycka, K., & Kowalczuk, P. (2024). Estimation of net accumulation and removal of fluorescent dissolved organic matter in different Baltic Sea water masses. Frontiers in Marine Science, 11, 1379604. https://doi.org/10.3389/fmars.2024. 1379604
- van de Velde, S. J., Hylen, A., Kononets, M., Marzocchi, U., Leermakers, M., Choumiline, K., et al. (2020). Elevated sedimentary removal of Fe, Mn, and trace elements following a transient oxygenation event in the eastern Gotland Basin, central Baltic Sea. *Geochimica et Cosmochimica Acta*, 271, 16–32. https://doi.org/10.1016/j.gca.2019.11.034
- Wikner, J., & Vikstrom, K. (2023). Extensive prokaryotic maintenance respiration in the sea influenced by osmoregulation. Frontiers in Marine Science, 10, 1070070. https://doi.org/10.3389/fmars.2023.1070070
- Williams, P. J. (1995). Evidence for the seasonal accumulation of carbon-rich dissolved organic material, its scale in comparison with changes in particulate material and the consequential effect on net CN assimilation ratios. *Marine Chemistry*, 51(1), 17–29. https://doi.org/10.1016/0304-4203(95)00046-t
- Wuttig, K., Heller, M. I., & Croot, P. L. (2013). Pathways of superoxide (O<sub>2</sub>-) decay in the eastern tropical North Atlantic. *Environmental Science and Technology*, 130826150409004. https://doi.org/10.1021/es401658t
- Yuasa, K., Shikata, T., Kitatsuji, S., Yamasaki, Y., & Nishiyama, Y. (2020). Extracellular secretion of superoxide is regulated by photosynthetic electron transport in the noxious red-tide-forming raphidophyte Chattonella antiqua. Journal of Photochemistry and Photobiology B: Biology, 205, 111839. https://doi.org/10.1016/j.jphotobiol.2020.111839
- Zhang, T., Hansel, C. M., Voelker, B. M., & Lamborg, C. H. (2016). Extensive dark biological production of reactive oxygen species in brackish and freshwater ponds. *Environmental Science & Technology*, 50(6), 2983–2993. https://doi.org/10.1021/acs.est.5b03906
- Zweifel, U. L., Wikner, J., Ake, H., Lundberg, E., & Norrman, B. (1995). Dynamics of dissolved organic carbon in a coastal ecosystem. Limnology & Oceanography, 40(2), 299–305. https://doi.org/10.4319/lo.1995.40.2.0299

TAENZER ET AL. 15 of 15